

Metrology and Optical Characterization of PECVD (RF) low temperature deposited Amorphous Carbon films.



F. Ferrieu¹, C. Chaton², D. Neira¹, C. Beitia³, L. Proenca Mota¹, A.M. Papon², A. Tarnowka⁴.

¹ STMicroelectronics, 850 rue Jean Monnet, F-38926 Crolles, France.

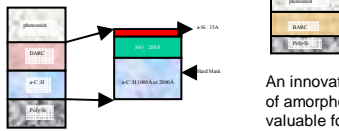
² CEA-LETI MINATEC, 17 rue des Martyrs, 38054 Grenoble cedex 09, France

³ KLA-Tencor, 32 chemin du vieux chène, 38240 Meylan, France

⁴ NXP, 850 rue Jean Monnet, F-38926 Crolles, France

For gates patterning in the 90 nm technology node, a stack composed of resist and spin on organic BARC is used. BARC has a very important role: it minimizes the substrate reflectivity to less than one percent, discards diffraction patterns, leading to better etch profile. BARC provides a mean to achieve dimensional control.

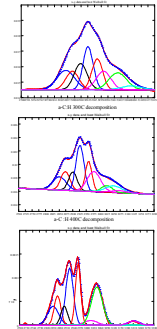
Figure 1 : gate 90 nm patterning stack. Resist budget (resist thickness necessary to achieve etch process) must be decreased otherwise fall of the resist, induced by the high aspect ratio, can occur.



An innovative solution can be developed involving the use of amorphous carbon (a-C:H) films. This material is valuable for the etch application in DRAM production

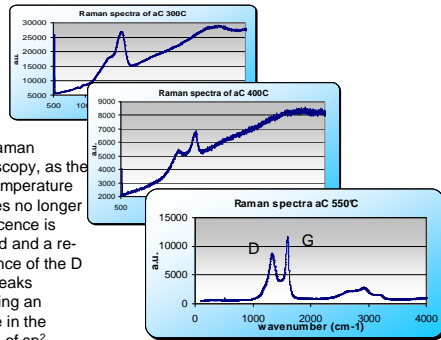
sample	%O +/- 0,2	%H +/- 1,5	%C +/- 1,7
a-C:H 300C 1500 Å	1.14	35.58	63.28
a-C:H 400C 1000 Å	1.7	37.83	60.47
a-C:H 400C 2000 Å	1	36	63
a-C:H 550C 2500 Å	1.18	25.42	73.4

• TABLE 1- Films compositions from correlated TOF SIMS, ERDA and RBS analysis of the samples, even at 550 °C deposition temperature there is still 25% hydrogen in the films. 550°C is close to the chemical hydrogenated desorption transition to the graphite state



sp² content is obtained by the IR spectra decomposition for each samples

From Raman spectroscopy, as the target temperature increases no longer luminescence is observed and a re-emergence of the D and G peaks suggesting an increase in the ordering of sp² bonded structures



The films Young E coefficient and Hardness have been measured with an MTS XPW nano-indenter, whereas density and stress were obtained from the stress curvature measurements method. The film thicknesses were determined from the X-Ray Reflectometry (XRR).

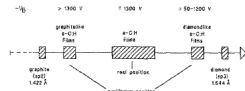
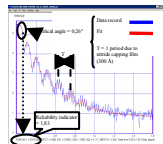
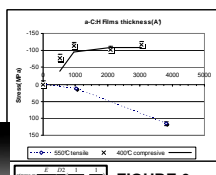
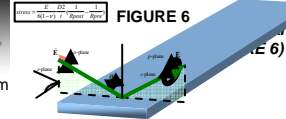


FIG. 15. Model of the phase transition of diamondlike to graphitelike a-C:H for the experiments concerning internal stress. On the abscissa the real atomic distances of neighboring carbon and the respective equilibrium distances during the transition are illustrated.

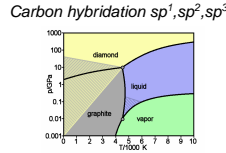
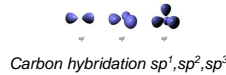


This transformation of compressive to tensile agree with the model of the phase transition but stress increases as

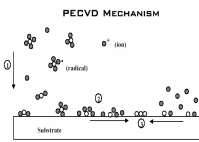
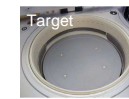


Spectroscopic Ellipsometry has been carried out using either the new VUV clean room tool from Kla-Tencor (150nm to 900nm). Other measurements were accomplished with our SE reference laboratory systems. The Spectroscopic Ellipsometry (SE) of a-C:H, was reported very early in 1983. The pioneer work was certainly from F.W Smith, (optical constants) [10], which consist of normal incidence reflectivity R and transmittance T measurements in the case of thick films DLC high temperature deposited samples. The EMA mixture between four known components: i.e., amorphous diamond like (sp³ bonds type), amorphous graphitic (sp² bonds), amorphous polymeric and void, have also been used later [11] with in situ and ex situ measurements for Diamond-Like Carbon, (DLC) materials. A similar analysis at 785°C was reported [12], with EMA mixing of Glassy C and sp² C in diamond. But these samples are made at a much higher temperatures, i.e. above 600°C, e.g. above the release of H bonds at 530°C [13].

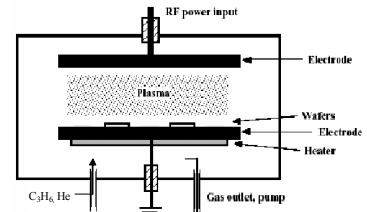
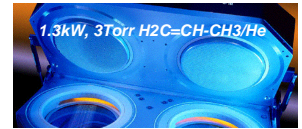
With amorphous nature of a-C:H films, Forouhi Bloomer and the Tauc Lorentz models are the most extensively used[14-17]. In theory the band gap energy E_g, related to the number of graphitic clusters present in the material, could be extracted... But simpler models have been used as well such as Lorentz oscillators. Increasing the numbers of these oscillators leads to perfectly adjusted. But Nevertheless it is now generally accepted that the best fit with experiment was by accounting with an uniaxial anisotropy. The origin of this anisotropy is somehow controversy. It can be seen as plain or partially oriented graphitic planes perpendicular to the substrate and has been detected from TEM pictures in ref [4] , a result somehow different from our observations (see HRTEM observation of the 550°C sample). Several questions remain however unanswered: the reason why an anisotropic model is more appropriate, even in the low temperature range, when the amorphous polymers-like nature of low temperature films a-C:H is observed



Carbon T/ Pressure phase diagram



Film growth involves surface reactions with incoming gas radical molecules. Radical concentration gradient drives the diffusion process. The net result from the fragmentation, the free radicals, and the ion bombardment (DC self bias voltage) enhances the surface processes and deposition occurs at much lower temperatures than in non-plasma systems



HRTEM Observation has been carried out using an Akashi EM002B Electron Microscope running at 200kV.. Two samples of a-C:H, 100nm thick covered with a lithography resist have been considered. The observation remains delicate since often the electron beam degrades the film. A very low contrast is observed between the resist layer and the Amorphous Carbon film in the a-C:H 400°C sample. On the contrary, the TEM observations of the 550°C sample clearly show the resist interface.

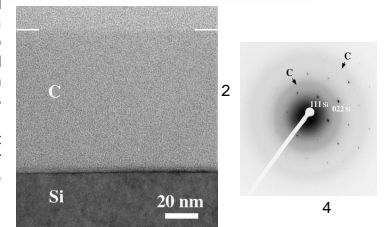
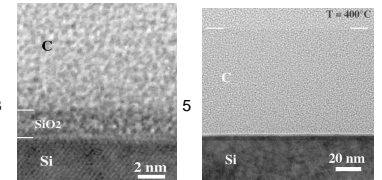


FIGURE 2 - X-Section of a-C:H films XTEM observation: upper carbon layer limit is depicted by white continuous lines on both sides.

FIGURE 3 - In a high resolution picture where the native oxide layer, (2nm-thickness), appear together with the silicon substrate lattice fringes, the a-C:H film morphology remains amorphous without evidence of polycrystalline. from also the transmission electron diffraction (FIGURE 4). For the 400°C sample

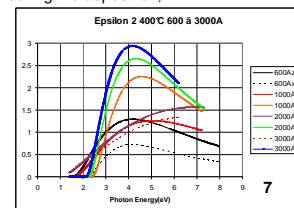


A weak contrast is observed between the a-C:H film and the resist layer FIGURE 5, indicating the material density change between 400 and 550°C as seen also in TABLE 2.

recipe	target	XRR mean	XRR density	mass pre (g)	mass post (g)	layer (g)	layer (nm)	mass density	Rpre	Rpost	thickness wafer	stress wafer	extrapolated thickness	stress calc
AC 600A	600	511.5	1.27	127.33032	127.33465	0.00433	4.327	1.2	-345.98	-324.89	0.771	-55.84	600	-65.5
AC 1000A	1000	932.8	1.26	127.30538	127.31336	0.00797	7.971	1.21	-352.69	-299.67	0.771	-91.356	1000	-97.94
AC 2000A	2000	2051.2	1.28	127.32127	127.33882	0.01754	17.544	1.21	-350.99	-260.60	0.771	-88.105	2000	-85.91
AC 3000A	3000	2994.6	1.27	127.33142	127.35693	0.02511	25.509	1.21	-345.63	-220.6	0.771	-97.64	3000	-97.82
ACL 1000A	1000-550*	1008.9	1.44	127.24593	127.25665	0.00971	9.712	1.36	-299.68	-305.44	0.771	10.821	1000	10.73
ACL 4000A	4000-550*	3786.2	1.45	127.32684	127.36373	0.03709	37.080	1.30	-299.25	-782.44	0.771	92.142	4000	97.34

TABLE 2 XRR results and stress curvature measurements a-C:H films, densities are expected approximately 1.3 to 2.0 g cm-3 [7]. The glassy carbon has a much lower density value, about (1.5 g.cm-3) whilst that of hydrocarbon polymers is about 1.0g.cm-3.

As shown in FIGURE 7, one also observes in this glassy state an increase of the birefringence as the thickness is increasing. Stress (compressive or tensile) during the deposition,



as well as when thickness is increased, induces preferred orientation in carbons films. Due to the elastic properties of the Amorphous Carbon network [17], the material undergoes reorientations at the molecular level, (only seen by optics, infrared and Raman spectroscopy). This demonstrates that as soon as the molecular dynamics of the Amorphous Carbon network can be modified by strain during the process [17], preferred orientation. A strain birefringence exist which has to be considered in the metrology



REFERENCES
 1. D. Neira, L. Proenca, L. Wang, M. Sanchez, C. Koenig and F. Ferrieu, *Microelectronic Packaging* (2015) Vol. 2015, pp. 481-487.
 2. M. Vogl, M. Steiner, H. Speth, *Electronical Science, Proceedings volume* (2005) 278.
 3. J. Linn, J. Chien, H. Chen, C. Schaefer, K. Liu and S. J. Pennycook, *Science*, 2015.
 4. S. Scherer, W. Q. Lu, B. G. Gowenlock, J. Edwards, J. Carter and T. S. Rossell, *Appl. Phys. Lett.* (2007).
 5. A. G. S. Filho, *Appl. Phys. Lett.* (2007).
 6. J. Robertson, *Carbon*, New York, Wiley, 1992, pp. 201-281.
 7. A. R. Kanehisa and S. R. Paul, *Appl. Phys. Lett.* (1983) 43, 120-122.
 8. X. Jiang, J. W. Zou, K. Ren and P. Guo, *Appl. Phys. Lett.* (1999) 75, 4723.
 9. F. W. Smith, *Appl. Phys. Lett.* (1983) 43, 120-122.
 10. B. Heng, *Appl. Phys. Lett.* (1983) 43, 120-122.
 11. S. Logothopoulos, *Phys. Rev. B* (1990) 42, 10200-10205.
 12. S. Logothopoulos, *Phys. Rev. B* (1990) 42, 10200-10205.
 13. Y. S. Lee, *Appl. Phys. Lett.* (1990) 56, 1020-1022.
 14. J. Robertson, *Carbon*, New York, Wiley, 1992, pp. 201-281.
 15. J. Robertson, *Carbon*, New York, Wiley, 1992, pp. 201-281.